Journal of Hydrology 565 (2018) 599–613

Contents lists available at ScienceDirect

Journal of Hydrology

journal homepage: www.elsevier.com/locate/jhydrol

Research papers

Performance evaluation of hydrological models using ensemble of General Circulation Models in the northeastern China

Muhammad Abrar Faiz[a], Dong Liu[a,b,c,d,*], Qiang Fu[a,*], Mo Li[a], Faisal Baig[e], Adnan Ahmad Tahir[f], Muhammad Imran Khan[g], Tianxiao Li[a], Song Cui[a]

[a] School of Water Conservancy & Civil Engineering, Northeast Agricultural University, Harbin, Heilongjiang 150030, China
[b] Key Laboratory of Effective Utilization of Agricultural Water Resources of Ministry of Agriculture, Northeast Agricultural University, Harbin, Heilongjiang 150030, China
[c] Heilongjiang Provincial Collaborative Innovation Center of Grain Production Capacity Improvement, Northeast Agricultural University, Harbin, Heilongjiang 150030, China
[d] Key Laboratory of Water-Saving Agriculture of Ordinary University in Heilongjiang Province, Northeast Agricultural University, Harbin, Heilongjiang 150030, China
[e] Department of Agricultural Engineering, Bahauddin Zakariya University, Multan, Pakistan
[f] Department of Environmental Sciences, COMSATS University Islamabad (CUI) – Abbottabad Campus, University Road, Tobe Camp, Abbottabad 22060, Pakistan
[g] Faculty of Agricultural Engineering, Department of Irrigation and Drainage, University of Agriculture Faisalabad, Pakistan

ARTICLE INFO

This manuscript was handled by Emmanouil Anagnostou, Editor-in-Chief, with the assistance of Alin Andrei Carsteanu, Associate Editor

Keywords:
General Circulation Models
Hydrological models
Climate change
Songhua River Basin

ABSTRACT

The Songhua River Basin (SRB) plays a vital role in supplying water resources to northeast China. This river has a substantial effect on agricultural grain producing region. Therefore, the current study was carried out to evaluate the performances of multiple hydrological models driven by bias corrected precipitation estimates from a group of General Circulation Models (GCMs). The variations in discharge obtained from multiple hydrological models were also analyzed. For this purpose, bias correction methods for GCMs and five hydrological models, lumped rainfall runoff (Nedbor Afstromnings Model (NAM), GRJ4), semi-distributed (the Water Evaluation and Planning tool (WEAP), HBV), and the distributed (Soil Water Assessment Tool (SWAT)) were used in the SRB. Before applying the bias correction method, raw GCMs were also plotted against observational data. The results revealed that none of GCM performed well against observational data. The results also showed that quantile mapping method corrects the biases of GCMs better than daily and monthly scale factors. Distributed and semi-distributed hydrological models performed better than lumped rainfall runoff models in the selected study area of SRB. By forcing hydrological models with bias corrected precipitation data, the differences in the simulated discharge by SWAT, HBV, NAM, GR4J and WEAP were −3%, −2%, −4%, −7 and +3, respectively, when compared with observed discharge. The results also show that the overall performance of SWAT, HBV, NAM, and WEAP was better than GRJ4. The results also suggest that the application of multiple hydrological models is necessary to make improvements in the planning and management of agricultural and water resources in the SRB region.

1. Introduction

Scientists and researchers worldwide agree that the global climate is warming, and that warming will have major effects on the hydrological cycle. After the 1950s, unprecedented changes began to be observed in global climatic conditions (Intergovernmental Panel on Climate Change (IPCC, 2014). Moreover, emissions of greenhouse gases are also contributing to altering the earth's climate and the hydrological cycle. The anticipated changes in climate variables are expected to change the magnitude and frequency of hydrological and climatic extremes in different regions (Giuntoli et al., 2015; Hagemann et al., 2013; Pokhrel et al., 2014; Teklesadik et al., 2017). Despite the availability of state-of-art hydrological models and global circulation models (GCMs), the current emphasis of the effects of climate on water resources has dealt with the inherent structure of hydrological models and the related parameters and downscaling methods.

Generally, GCMs represent conditions related to biogeochemical processes, land surface, ocean, cryosphere and atmosphere on a geographical grid, which covers the globe. Different GCMs use different climate modeling systems that depend on the representative institute which provides the related data. This means that the greenhouse gas scenario and spatial resolution of the GCMs differ for the different

* Corresponding authors at: School of Water Conservancy & Civil Engineering, Northeast Agricultural University, Harbin, Heilongjiang 150030, China.
E-mail addresses: liudong@neau.edu.cn (D. Liu), fuqiang@neau.edu.cn (Q. Fu).

https://doi.org/10.1016/j.jhydrol.2018.08.057
Received 17 October 2017; Received in revised form 13 August 2018; Accepted 25 August 2018
Available online 30 August 2018
0022-1694/ © 2018 Elsevier B.V. All rights reserved.

GCMs; this fact restricts the direct application of GCMs at local and regional scales, and particularly impacts the study of the effects of climate change on hydrology and the environment (Wilby et al., 2000). Different downscaling methods, such as statistical and dynamic methods have been developed to correct the biases found in GCMs and to reduce higher resolution GCM output to smaller or site scales (Hay and Clark, 2003; Wetterhall et al., 2006). The statistical downscaling methods based on statistical relationships between local /regional variables and large scale climate information, while dynamical downscaling methods employ regional climate models (RCMs) for limited regions with boundary conditions from GCM simulations (Maraun et al., 2010; Wilby et al., 2004). These RCMs with higher resolutions are able to capture smaller scale process more realistically. The dynamic downscaling methods guarantee consistency with the GCM and models output variables internally consistent. These methods are developed for RCMs to study wave energy resource evaluation, flooding risks assessment, complex costliness and complex topography (Laugel et al., 2014; Tian et al., 2013). But the disadvantage of dynamic downscaling is an intensive computation required to run a single scenario while statistical downscaling provides a simple and faster method for the computation required to run large scale GCMs. Therefore, most researchers and scientists have used statistical downscaling techniques to study the effects of climate change on hydrological and environmental behavior (Giuntoli et al. 2015; Wetterhall et al. 2006; Wilby et al. 2000). Recently, some researchers have developed statistical models and bias correction techniques that have also been reported in literature such as the Lars weather generator, statistical downscaling model and automated statistical downscaling model, power transformation, linear scaling, and distribution mapping (Hessami et al., 2008; Li et al., 2013; Semenov and Barrow, 1997; Teutschbein and Seibert, 2012; Wilby et al., 2000). However, these models only downscale HadCM3-A2 and CanCM3-B2 scenarios of the 4th Assessment Report of the IPCC because the restrictions on models to successfully make predictors and then link with predictands. In bias correction methods, usually two steps are adopted: (1) observed and simulated data are used to determine the scale factors, and (2) adjustment of simulated GCMs is employed with acquired scale factors to remove biases. In the aforementioned techniques, the calculation of scale factors is an important task. The details of calculating scale factor are presented in Section 3.1.

In addition to bias correction of GCMs, past researches have also applied GCMs and multiple hydrological models at regional and local scales to study the impact of climate change caused by differences between the structure of hydrological models and their parameters (Giuntoli et al., 2015; Hagemann et al., 2013; Jiang et al., 2007). Gosling et al. (2011) documented that the difference in mean annual discharge depends on the selection of a specific hydrological model. Their results exhibited up to a 25% difference in the annual modeled discharge and this difference was larger after the selection of GCMs than after the selection of a hydrological model. Poulin et al. (2011) found significant uncertainty existed in hydrological model structure than in the uncertainty of hydrological model parameters. Likewise, precipitation and land use have also affected the runoff. For example, (BI et al., 2009; Yin et al., 2017) studied the effect of land use and precipitation in different parts of China and documented a significant influence of land use changes on runoff. Fang et al. (2012) found erosive effect of rainfall characteristics in the Wangjiaqiao watershed. As summarized above, quantifying studies are very important for decision making related to water resources and agricultural management. A recommendation based on a single hydrological model may be highly uncertain whereas the use of multiple hydrological models and their combination with GCMs would highlight different sources of uncertainty and this can help decision makers to take appropriate mitigation measures before the occurrence of a natural hazard such as a flood or drought.

Several studies have been carried out in the Songhua River Basin (SRB) in northeastern China to assess the effects of climate variables and changes in water resources (Faiz et al., 2017a; Faiz et al., 2017b; Liu et al., 2016; Mu et al., 2012; Song et al., 2015). Scientists have usually reached a consensus that temperature is rising while changes in precipitation remain uncertain in the SRB. For example, Song et al. (2015), Khan et al. (2016), and Faiz et al. (2018) studied the historical trend of precipitation, temperature in the SRB and documented that the precipitation has an increase and decrease trend while temperature has risen from 1 to 1.5 °C in last five decades at 82% stations. In the literature, several studies in the SRB have dealt with changes in precipitation projected by GCMs but a literature gap of ensembles of GCMs exists with hydrological models in the SRB. Because stream flow is very sensitive to changes in precipitation, the ambiguity in projected stream flow will complicate the future planning and management of water resources in this region.

The studies cited above mostly used non-parametric trend tests to assess the changes in river discharge and climate variables (such as precipitation). Although non-parametric trend tests are sufficient to represent the best state-of-art methods for determining changes in river discharge and precipitation. But during an impact evaluation study, quantifying the contributions of climate variables (e.g., precipitation), an ensemble of multiple hydrological models and GCMs should be used to provide a more reliable assessment of changes in river discharge.

In the context of the above literature, three hydrological models, the GR4J lumped precipitation–runoff model, water evaluation and planning tool (WEAP), a conceptual rainfall runoff NAM model, Hydrologiska Byråns Vattenbalansavdelning (HBV), and Soil Water Assessment Tool (SWAT) along with the bias corrected precipitation obtained from an ensemble of seven GCMs were used to analyze conditions in the SRB of northeastern China. The main goals of the study were:

1. To evaluate the performance of the GR4J, WEAP, NAM, HBV, and SWAT models under current climate conditions in the SRB.
2. To examine the reliability of the GR4J, WEAP, NAM, HBV and SWAT models forced by downscaled precipitation of an ensemble of GCMs.

2. Study area

The SRB, the seventh largest major river basin in China, stretches between 41°42′–51°48′N, 119°52′–132°31′E with an area of 556,800 km^2. The SRB is divided into three sub-basins, (1) the main stream of the Songhua River, (2) the Second Songhua River and (3) the Nenjiang Basins. The Second Songhua River and the Nenjiang are the southern and northern sources of the main stream of the Songhua River, respectively (Mu et al., 2012).

The current study emphasized the main stream of Songhua River gauged at Harbin Gauging station that covers an area of 53,600 km^2 and is located in the middle of the SRB (Fig. 1). This sub-basin is the main agricultural area of the region and stands at an elevation of 80–1666 m a.s.l. The mean annual precipitation in the selected basin ranges from 400 to 700 mm while mean annual temperature ranges from 1 to 5 °C (Faiz et al., 2018; Song et al., 2015). According to Hydrological Bureau of Harbin, the mean monthly discharge at the Yilan Gauge station is 18,228 MCM.

The daily datasets for climate variables such as relative humidity, temperature (minimum and maximum), wind speed, precipitation, evaporation, and sunshine hours from 1961 to 2016 for ten climatic stations were obtained from the Harbin Metrological Department, Heilongjiang Province, China (Fig. 1). The quality of the data had already been reviewed by the Harbin Metrological Department.

The daily discharge datasets gauged at Yilan station for the period of 1988 to 2016 were also obtained from the Harbin Hydrological Department (Fig. 1). Moreover, historical outputs of seven GCMs with different resolutions for precipitation (1961 to 2005) and outputs of GCMs for the period of (2006 to 2010) under representative

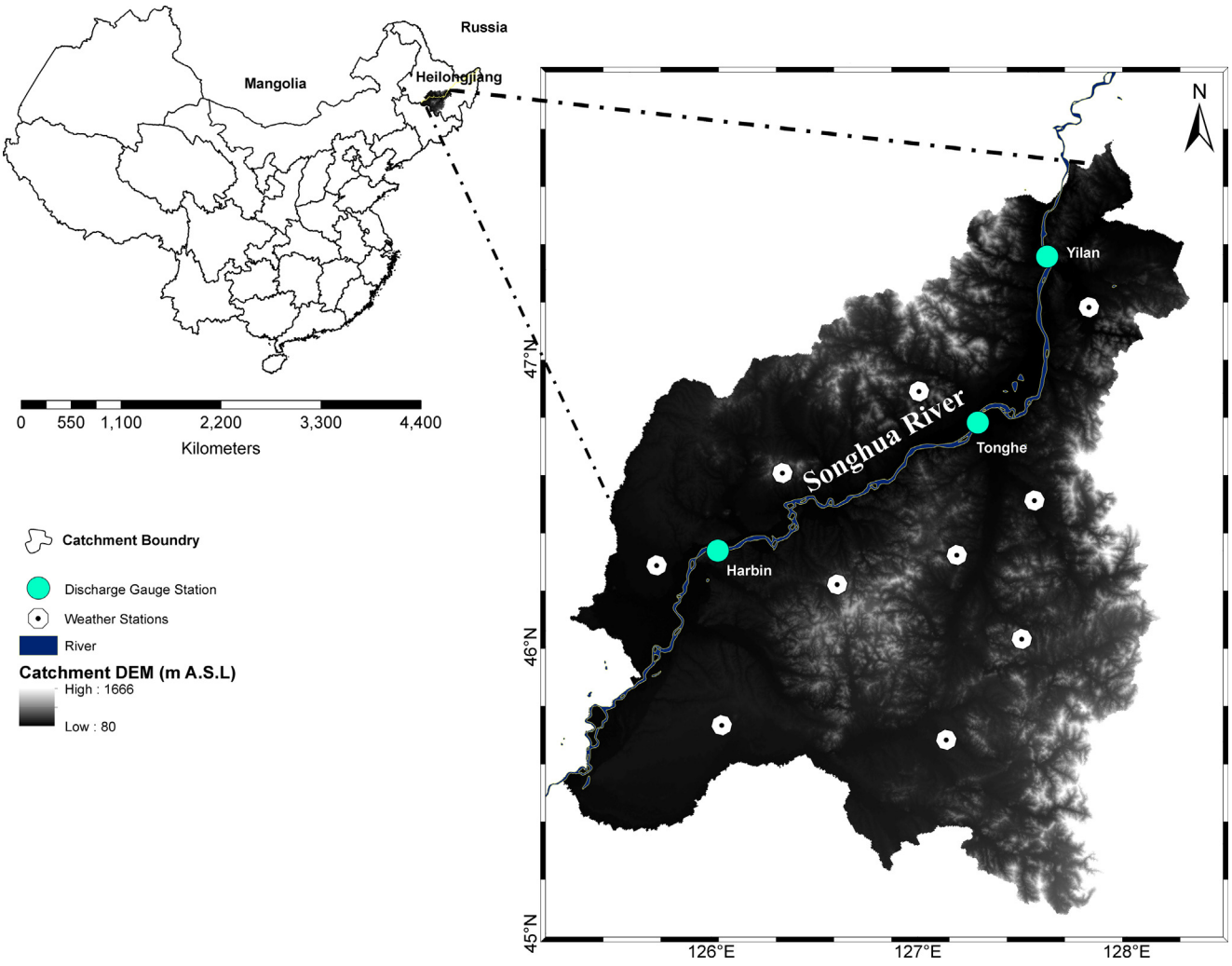

Fig. 1. Location of Songhua River Basin.

Table 1
Description of CMIP5 GCMs for which historical inputs and RCP 2.6, RCP 8.5 simulation results were available from ESG.

GCM	Center name	Model acronym	Resolution (longitude × latitude)
1	Beijing Climate Center, China Meteorological Administration, China	BCC-CSM 1.1m	1.125° × 1.125°
2	Beijing Normal University, China	BNU-ESM	2.812° × 2.812°
3	Canadian Centre for Climate Modeling and Analysis, Canada	CanESM2	2.812° × 2.812°
4	Institute Pierre-Simon Laplace, France	IPSL-CM5A-LR	3.75° × 1.875°
5	NASA Goddard Institute for Space Studies, USA	GISS-E2-H	2.5° × 2.0°
6	National Center for Atmospheric Research (NCAR), USA	CCSM4	1.25° × 1.25°
7	AORI, NIES, JAMSTEC, Japan	MIROC-ESM-CHEM	2.812° × 2.812°

concentration pathway 2.6 (RCP 2.6) from different institutes were also downloaded from https://pcmdi.llnl.gov/search/cmip5/, and these data were provided by the World Climate Research Program (Table 1). The RCP 2.6 represents the lowest RCP scenario (Rogelj et al., 2012). Therefore, in this study RCP 2.6 was taken for making ensemble of GCMs to force hydrological models for the period of 1988 to 2010. These seven models performed well during a previous evaluation and projection of future changes in precipitation and temperature in China (Sun et al., 2015).

3. Methods

3.1. Linear scaling

Section 1 discussed a few bias correction methods for GCMs that were needed because of their coarse resolution. However, linear scaling provides the simplest and easiest method of correcting the biases in GCMs; as a result, a number of researchers worldwide have used linear scaling for bias correction of RCMs and GCMs (Lenderink et al., 2007; Mahmood and Babel, 2013; Mahmood and Shaofeng, 2016; Piani et al., 2010a, 2010b). With these correction methods, authors usually calculate scale factors on a monthly basis, which limits its usefulness in exploring daily variations in the data.

In the modified linear scaling method, the temporal resolution of scaling factors increased during the transition from a monthly to a daily basis by using Eq. (1):

$$P_{c_daily} = P_{raw_daily} \times \frac{\mu(P_{obs_daily})}{\mu(P_{raw_daily})} \quad (1)$$

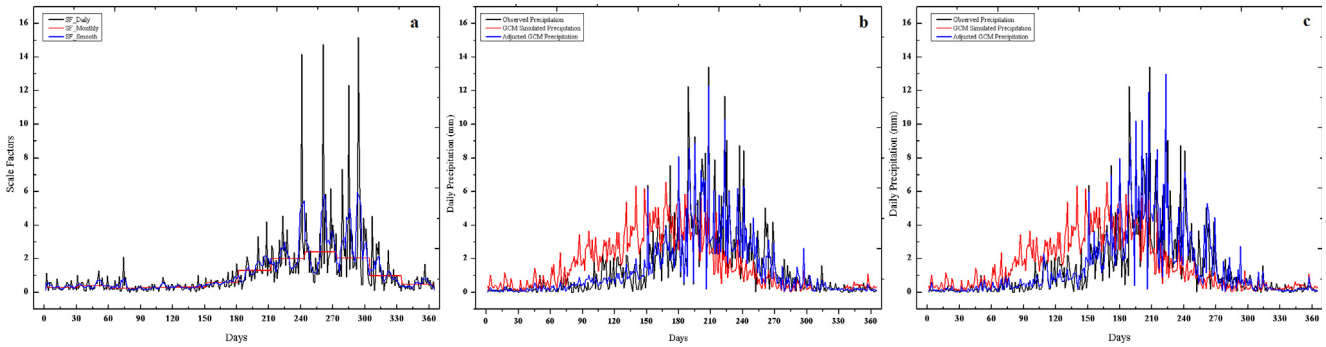

Fig. 2. (a) Calculation of scaling factors with original linear scaling (black line) and modified linear methods (blue line after smoothing and red line with monthly scale factors after smoothing) for SRB (1961–1975), (b) application of calculated monthly scale factors for BCC-CSM 1.1 (m) model (c) application of calculated daily scale factors for BCC-CSM 1.1 (m) model in the SRB. (For interpretation of the references to colour in this figure legend, the reader is referred to the web version of this article.)

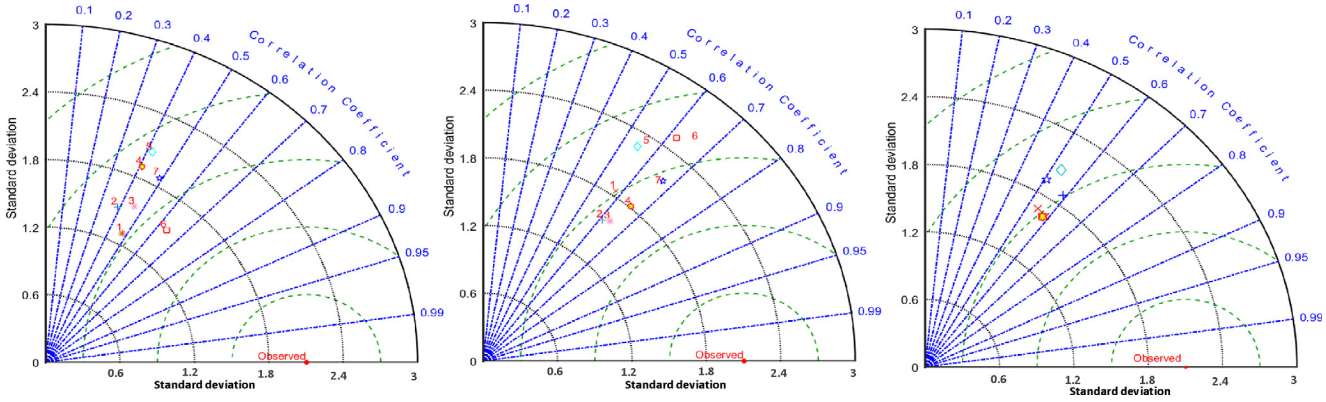

Fig. 3. Taylor diagram for GCMs before correction (left), after applying daily scale factors (middle), and by quantile mapping (right).

where P_{c_daily} is the corrected daily precipitation time series for any period (e.g., 1990–2005); P_{raw_daily} is the raw daily precipitation simulated by a GCM for the period 1990–2005; P_{obs_daily} is the daily observed precipitation for the control period (e.g., 1961–1975); and μ is the expectation operator; for example $\mu(P_{obs_daily})$ is the average value of precipitation for a given day. In this proposed method, 365 scales factors "$\frac{\mu(P_{obs_daily})}{\mu(P_{raw_daily})}$" were obtained from long-term daily observed precipitation and GCM precipitation, instead of 12 scaled factors. Intensive care is required at the time of calculating scale factors, because they depend on the annual cycle of a GCM.

Before applying the corrected precipitation data to hydrological models, the modified linear scale method was used to evaluate the observed precipitation data. For this purpose, the observed and GCMs data were divided into two sets, a control and the scenario periods as defined above. Then, mean daily scale factors for the control period were obtained by applying the formula "$\frac{\mu(P_{obs_daily})}{\mu(P_{raw_daily})}$". Before applying these scale factors using Eq. (1), a Gaussian filter (Mitchell et al., 1966) was applied by MATLAB to smooth the scale factors. Different filters such as running average, low, high and band pass filters can be used to smooth data (Chatfield, 2016). In Gaussian filter the standard deviation of the Gaussian distribution can be related to 50% of frequency response of the filter. Therefore an appropriate Gaussian distribution has standard distribution $\sigma_G = \frac{\lambda_{0.5}}{6}$ ($\lambda_{0.5}$ is desired wave length). The weights of the filter can be obtained by sampling the probability distribution functions of the standard normal distribution at t-values 0, $\pm 1/\sigma_G$, $\pm 2/\sigma_G$, $\pm 3/\sigma_G$. ... In this study, a wavelength of 30 years is taken to get a Gaussian filter with frequency response of 0.5. For more detail of application of Gaussian filter we refer readers to the paper of (Mitchell et al., 1966). Furthermore, the monthly scale factors "$\frac{\mu(P_{obs_monthly})}{\mu(P_{raw_monthly})}$" were also calculated to find the difference in downscaled data, see Fig. 2a. For clarification, it could be seen that from days 180 to 270, the monthly scale factors ranged from 1.7 to 2.2, while daily scale factors have different ranges. This indicate that correction of GCMs with monthly scale factors for a particular month might correct the mean values of that month but there might be different daily values for that month.

Finally, smooth scale factors were adjusted with daily precipitation of each GCM to obtain the correct GCM data for each station in the SRB. A graphical presentation of the corrected precipitation by daily scale and monthly factors for the BCC-CSM 1.1 (m) model is presented (Fig. 2b, c). The corrected precipitation with daily scale factor is more consistent and accurate compared to monthly scale factors. For more robust assessment, the corrected precipitation determined by the modified linear scaling method (based on daily scale factors) was also evaluated using a Taylor diagram. A Taylor diagram is a brief summary of the evaluation of the observed and simulated data in terms of the root-mean-square difference, correlation and ratio of variances (Taylor, 2001). The results show that the corrected daily precipitation data had good agreement and correlation between the observed and downscaled precipitation (Fig. 3).

3.2. Quantile mapping

The quantile mapping (QM) is a non-parametric bias correction method. This method is applicable for distributions of precipitation without any assumption on precipitation distribution. This particular bias correction approach is based on empirical transformation and successfully implemented to correct the biases of RCMs precipitation (Fang et al., 2015; Jakob Themeßl et al., 2011; Sun et al., 2011). The effective advantage of this method is to correct biases in quantiles, wet-day frequency, mean and standard deviation. The bias correction of

Table 2
Brief description of three hydrological models.

Model	Source	Method Runoff Routing	Input climate parameters	Method: potential evapotranspiration	Model Family	Parameters
GR4J	https://webgr.irstea.fr/modeles/journalier-gr4j-2/?lang=en	Based on interception, production store and routing store	Precipitation, Potential evapotranspiration, Stream Flow	Penman-Monteith	lumped precipitation–runoff model	Four parameters from X1 to X4 [Interception, soil storage, flood tracking (Routing store) to calculate the rainfall-runoff process]
WEAP	http://www.weap21.org/index.asp?action=40 License version	one dimensional, 2-compartment (or "bucket") soil moisture accounting scheme is based on empirical functions that describe evapotranspiration, surface runoff, sub-surface runoff (i.e., interflow), and deep percolation	Precipitation, Temperatures (min. and Max.), relative humidity, wind speed and Stream Flow	Penman-Monteith	Soil moisture accounting model	Root zone soil water capacity, Root zone conductivity, Deep water capacity, Deep conductivity, Runoff resistance factor (includes LAI)
NAM	Department of Agricultural Engineering, BZU, Pakistan	Saint- Venant equations	Precipitation, Temperatures (min. and Max.), relative humidity, wind speed and Stream Flow	Penman-Monteith	lumped rainfall-runoff conceptual model	Maximum water content in surface storage, Maximum water content in lower zone/root storage, Overland flow coefficient, Interflow drainage constant, Overland flow threshold, Interflow threshold, Groundwater recharge threshold, Timing constant for overland flow, Timing constant for interflow, Timing constant for base flow
HBV	https://www.mathworks.com/matlabcentral/fileexchange/41395-hbv-edu-hydrologic-model	Based on lime lag method	Precipitation, Temperature and Stream flow	Blaney-Criddle	lumped (semi-distributed) daily rainfall-runoff model	Maximum soil moisture, Soil moisture threshold for reduction of evaporation, Shape coefficient, recession coefficient, Threshold for outflow, Maximal flow from upper to lower ground water box, Routing, length of weighting function
SWAT	http://swat.tamu.edu/ Analysis: laboratory of Department of Agricultural Engineering, BZU, Pakistan	Muskingum method	Precipitation, Temperature and Stream flow	Penman-Monteith, Hargreaves, Priestely-Talyor	Distributed model	The runoff curve number, Groundwater delay time, Base flow alpha factor, Groundwater "revap" coefficient, Threshold depth of water in the shallow aquifer required, Base flow alpha factor for bank storage, Effective hydraulic conductivity in main channel alluvium, Snowfall temperature, Manning's "n" value for the main channel

Table 3
Evaluation of seven GCMs (without Correction) with mean daily precipitation for the period of 1961–1990, in the Songhua River Basin.

Models	Obs_mean	Obs_Std.	Model_mean	Model_Std.	E_mean	E-Std.	R
BCC-CSM 1.1(m)	1.5	4.2	1.7	3.8	−0.2	0.4	0.10
BNU-ESM	1.5	4.2	1.7	3.6	−0.2	0.6	0.09
CanESM2	1.5	4.2	1.7	3.3	−0.2	0.9	0.12
CCSM4	1.5	4.2	2.2	3.3	−0.7	0.8	0.14
GISS-E2-H	1.5	4.2	1.9	4.0	−0.4	0.1	0.12
IPSL-CM5A-LR	1.5	4.2	2.2	3.3	−0.7	0.8	0.14
MIROC-ESM-CHEM	1.5	4.2	2.4	4.4	−0.8	−0.3	0.10

Obs_mean: observed mean value, Obs_Std. Observed standard deviation, Model_mean: Model mean value, Model_Std. Model standard deviation E_Mean: error between observed and Model mean, E_Std. error between observed standard deviation and Model standard deviation, R: correlation coefficient.

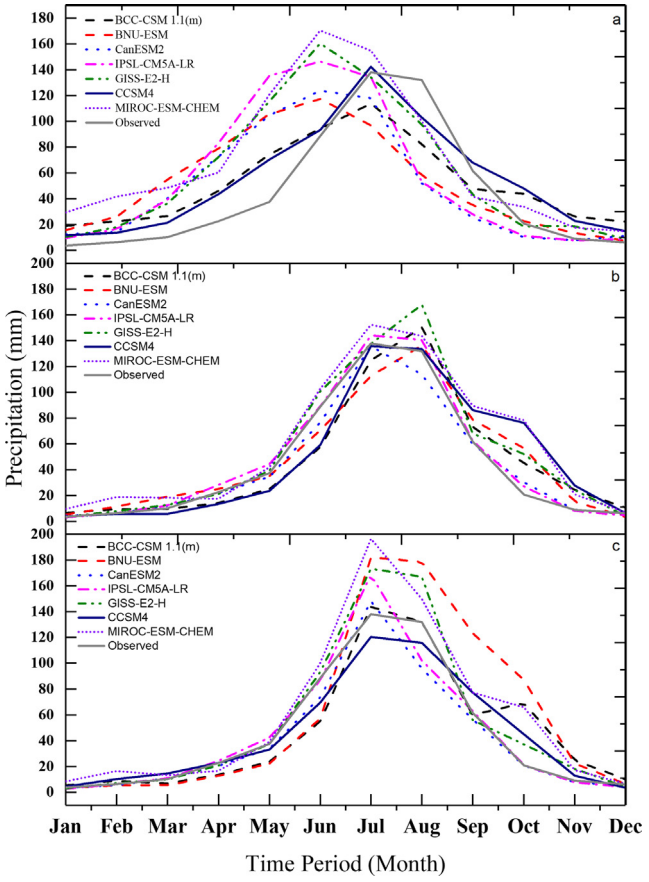

Fig. 4. Comparison of GCMs at monthly scale (a) without correction, (b) correction by daily scale factors, (c) correction by monthly scale factors.

GCMs based on quantile mapping can be expressed based on empirical distribution function and inverse of empirical distribution function (Fang et al., 2015; Gudmundsson et al., 2012; Piani et al., 2010a, 2010b);

$$P_{correct_daily} = ecdf^{-1}_{obs_month}(ecdf_{raw_month}(P_{raw_daily})) \quad (2)$$

where $ecdf^{-1}_{obs_month}$ represents the inverse cumulative distribution function of mean value of observed precipitation at given month m; $ecdf_{raw_month}$ represents cumulative distribution function of mean value of non-corrected GCM simulated precipitation at given month m, and P_{raw_daily} is the raw daily precipitation simulated by a GCM at a given month.

3.3. Hydrological models

The hydrological conditions in the SRB were modeled using five hydrological models: WEAP, NAM, GR4J, HBV and SWAT. These five models were selected because they employed different runoff routing methods. The brief description of each model and the related input parameters are summarized in Table 2. The hydrological models were forced with observational data and the precipitation simulated in an ensemble of seven GCMs including other climatic parameters that were fixed during the analysis such as temperature (minimum & maximum), relative humidity, and wind speed. The calibration (1988–2010) and validation (2011–2016) of the hydrological models were carried out by stream flow gauging at Yilan station that is located at the end of the main stream of the basin.

4. Results and discussions

4.1. Performance evaluation of raw GCMs

The performance of daily mean precipitation for the raw GCMs (without correction) for the period of 1961–1990 was evaluated by comparing that data with observed daily precipitation data. For this purpose, statistical indicators such as, (1) the correlation co-efficient (R); (2) error between mean of observed and GCM; and (3) error between standard deviations of observed and GCM were calculated for the entire study area. These statistical indicators were mostly used for performance evaluation of observational data against GCM data (Mahmood and Babel, 2013; Mahmood and Shaofeng, 2016). To investigate the basin-wide pattern of precipitation captured by GCMs, the mean monthly observational data and GCMs data were plotted by taking the arithmetic mean of the observed and all the GCMs grids that covered the basin.

The indicators were calculated based on daily time series raw precipitation data of seven GCMs against the observational data. All the GCMs predicted a correlation of less than 0.50. The remaining indicators exhibited poor performance of all GCMs in the region. The errors in standard deviation and errors in mean ranged from −0.3 to 0.90 mm/day and −0.2 to −0.8 mm/day, respectively (Table 3). The poor performance of GCMs shows that raw GCMs cannot be used for an analysis at either the basin or regional scale. The mean monthly precipitation of all seven GCMs against observed precipitation is presented in Fig. 4a. This graphical presentation revealed that somehow all models overestimated the predicted precipitation. Moreover, the performance of GCMs showed well agreement when bias corrected with daily scale factors compared to monthly scale factors (Fig. 4b & c).

4.2. Performance evaluation of GCMs by modified linear scaling and quantile mapping methods

According to the application of impact study, different statistics could be used for evaluation of downscaling or bias correction methods such as temporal characteristics or intensity metrics (Maraun et al., 2010). The mean, variance, percentile, percentage wet, wet and dry spell length, and peak over threshold are commonly used statistics for bias corrected precipitation (Chen et al., 2012; Khan and Coulibaly, 2010; Wetterhall et al., 2006). The statistics calculated for corrected

Table 4
Evaluation of ensemble of seven GCMs Correction for the period of 1961–1990, in the Songhua River Basin.

Indicators	Season	OBS	Bias Correction			Indicators	Season	OBS	Bias Correction		
			DSF	MSF	QM				DSF	MSF	QM
Mean	Winter	2.2	2.0	1.9	2.2	Max. dry spell Length	Winter	90.0	90.0	90.0	90.0
	Spring	4.8	2.8	2.4	4.2		Spring	54.0	45.4	42.7	51.9
	Summer	11.2	7.1	6.8	8.6		Summer	30.0	19.5	22.0	19.3
	Autumn	6.8	5.0	4.4	5.5		Autumn	46.0	48.0	45.3	44.0
	Annual	8.4	5.7	5.1	6.8		Annual	81.0	88.1	92.4	104.1
Variance	Winter	1.9	1.5	1.4	2.1	Max. Wet spell Length	Winter	3.0	3.1	3.1	3.6
	Spring	17.9	12.8	12.7	20.8		Spring	5.0	10.0	11.1	9.0
	Summer	169.3	114.9	125.9	122.4		Summer	7.0	13.0	18.0	17.0
	Autumn	68.7	46.2	36.2	51.4		Autumn	5.0	8.9	9.1	10.1
	Annual	114.5	73.4	67.6	86.5		Annual	8.0	20.1	11.1	17.1
Percentile	Winter	5.2	4.5	3.6	5.2	Peaks over threshold	Winter	0.0	0.1	0.0	0.0
	Spring	14.1	8.4	8.3	12.8		Spring	4.0	3.4	2.6	15.0
	Summer	36.9	20.9	24.2	29.4		Summer	144.0	206.3	206.6	180.9
	Autumn	21.9	16.9	16.5	18.3		Autumn	31.0	35.1	40.6	37.1
	Annual	28.3	19.4	17.3	23.1		Annual	179.0	229.5	241.9	233.0
Percentage Wet	Winter	0.0	0.0	0.0	0.0						
	Spring	0.1	0.2	0.2	0.2						
	Summer	0.3	0.6	0.6	0.5						
	Autumn	0.2	0.2	0.2	0.2						
	Annual	0.2	0.3	0.3	0.2						

Table abbreviations: OBS = observed, DSF = Daily scale factor, MSF = Monthly scale factor, QM = Quantile mapping.

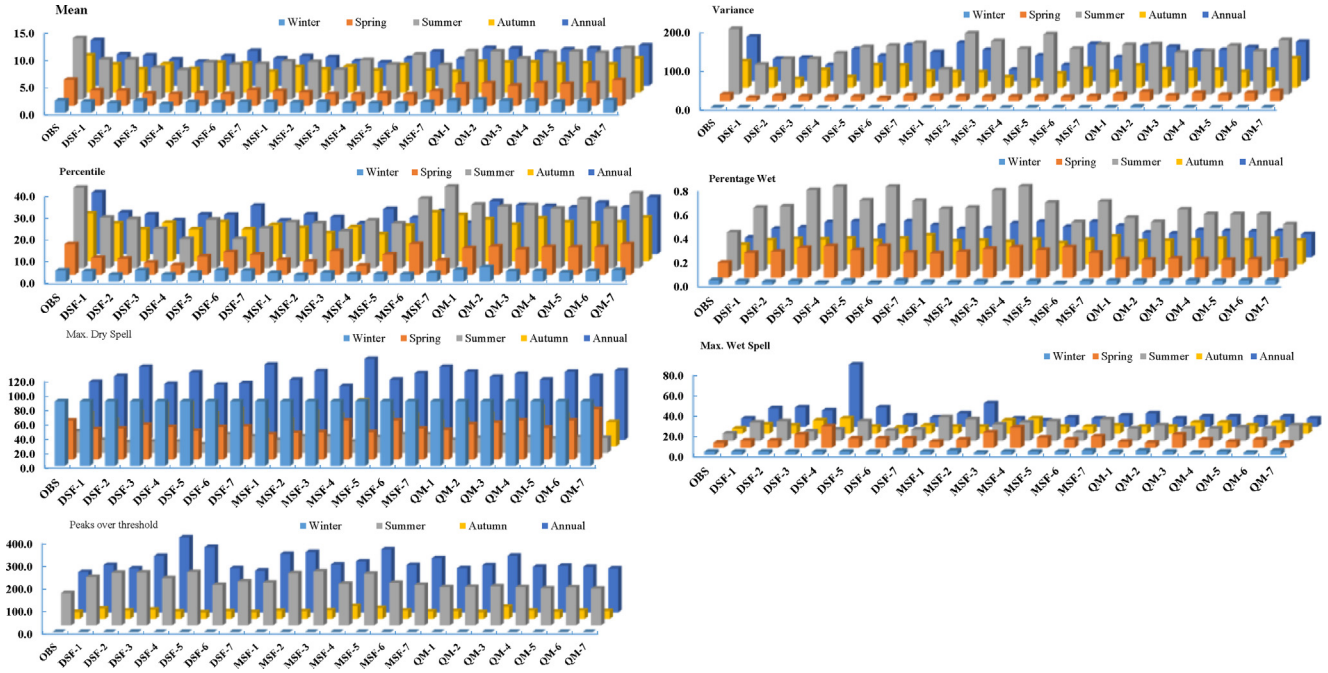

Fig. 5. Graphical representation of calculated statistics based on bias correction methods: Here DSF (daily scale factor), MSF (monthly scale factors, and QM (quantile mapping).

GCMs with modified linear scaling of mean daily and mean monthly precipitation as well as quantile mapping for the period of 1961–90 are presented in Table 4. The results demonstrate a good agreement between the corrected GCMs and observational data in the basin. The results indicate that means and variances were well improved when compared with raw GCMs. Even the corrected GCMs show better improvement when the statistics were calculated for quantile mapping method. To examine the performance of corrected versus observational data, the statistics for different seasons (winter, spring, summer, autumn, and annual) were also calculated. For this purpose, the precipitation threshold value was assumed 1.0 mm. It is evident that quantile mapping showed better performance than linear scaling. During analysis, it was observed that quantile mapping caused an overwhelming advantage to linear scaling, because most statistics exhibited better performance for quantile mapping than those of linear scaling (Table 4). For example, wet day percentage and maximum dry day spell in winter and summer, maximum wet day spell and peak over threshold in winter, spring and annual showed better statistics than linear scaling methods.

In the current analysis, precipitation corrected by daily scale factors was also compared with precipitation bias corrected by monthly scale factors (Table 4). The results indicate that daily scale factors exhibited an improvement in means and variances as well as percentage wet, based on the statistics calculated for the period of 1961–90

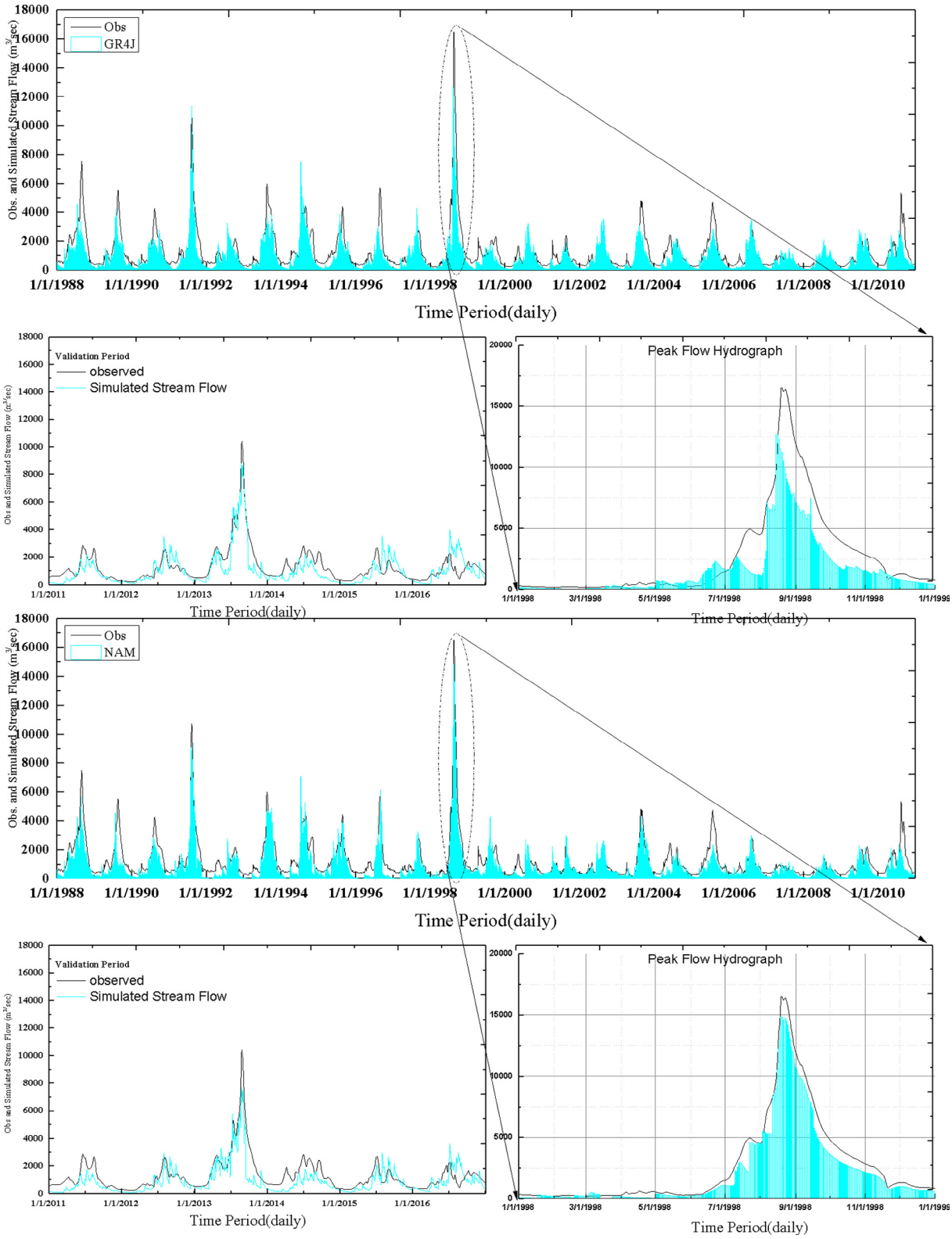

Fig. 6. Stream flow calibration and validation for the period of 1988–2016 by GR4J and NAM models.

precipitation time series. The main purpose of modification in linear scaling was to correct the daily variation in the precipitation time series. Although both linear scaling methods showed an overestimation in the most of statistics results, precipitation time series data corrected by daily scale factors somehow proved similar to the correction carried out by quantile mapping. The graphical presentation and statistics showed that the modified linear scaling method and quantile mapping performed better than original linear scaling and can be used in daily precipitation time series that are based hydrological models (Fig. 5).

Table 5
Models calibration and validation estimated parameter values.

Model	GR4J		WEAP		NAM		HBV		SWAT	
	NSE	R^2	NSE	R^2	NSE	R^2	NSE	R^2	NSE	R^2
Calibration 1988–20-10	0.62	0.67	0.83	0.86	0.73	0.80	0.80	0.86	0.81	0.82
Validation 2011–20-16	0.64	0.70	0.88	0.92	0.80	0.84	0.82	0.86	0.80	0.81

4.3. Calibration and validation of hydrological models using observational data

The performance of hydrological models (GR4J, WEAP, NAM, HBV, and SWAT) was checked for the SRB region based on observational data. Additionally, non-dimensional criteria such as Nash Sutcliffe efficiency (Nash and Sutcliffe, 1970) and Pearson correlation coefficient (Lee Rodgers and Nicewander, 1988) were also computed between observed and simulated runoff by using hydrological models. The predicted values were calibrated using correction factors that generate predicted values that were consistent with the observed values, while validation was done to judge the performance of each model using observational data that was not used during the calibration process and time period. In this study, the hydrological models are classified into two categories; (a) lumped rainfall runoff models, (b) semi-distributed and distributed hydrological models;

(a) **Lumped rainfall runoff models:** To evaluate the best performance of GR4J, the model was calibrated several times to obtain the best parameter values. If new parameters provided better results than the previous ones, the previous parameters were replaced by the new ones. This procedure continued until the best values were obtained. During the calibration period the Nash-Sutcliffe efficiency (NSE) was not greater than 0.62 for the period from 1988 to 2010. Likewise, during the validation period the NSE was never less than 0.64. The graphical representation of calibration and validation period is presented in Fig. 6. It was noted that GR4J model underestimates the peak flow, while low flow showed a little bit over estimate. This under and over estimation of flow directly related to model parameters. For example, during the calibration, it was observed that the parameter X4 which is related to unit hydrograph is most sensitive to high flows, while X2 that is related to groundwater is sensitive to low flows. The parameters X1 (production store) and X3 (routing store) were sensitive to target function (NSE), because target function is a statistical measure that calculate the performance of simulated and observed flows. The results suggested that sensitivity of these four parameters could not be ignored because all these parameters directly affect the hydrograph. Lerat et al. (2012) also confirm that stability of these four parameters is a primary importance at the time of applying GR4J in operational conditions. The NAM model was run for the same time period (1988–2010) to obtain the optimized parameter values for the basin. During calibration, the NSE value was obtained as 0.73; likewise, the value of NSE was found to be 0.80 for the validation period. During analysis, the correlation coefficient between observed and simulated data for NAM was never less than 0.80, while for GR4J the minimum correlation coefficient was found to be 0.70 (Table 5). During analysis, it was also observed that for the NAM model, the parameters for the

Table 6
Optimized parameter values during the time of calibration.

Model	Parameter	Definition	Calibrated Value
NAM	Umax (mm)	Max W.C in the surface storage	12
	Lmax (mm)	Max W.C in root zone storage	55
	CQOF	Overland flow runoff coefficient	0.32
	CKIF (hrs)	Time Constant for Interflow	588
	CK1,2 (hr)	Time constant for routing overland flow	16
	TOF	Root zone threshold value for overland flow	0
	TIF	Root zone threshold value for inter flow	0.1
	CKBF (hr)	Time constant for routing base flow	2520
	Tg	Root zone threshold value for groundwater recharge	0.8
WEAP	Root zone soil water cap (mm)	–	2500
	Root zone conductivity (mm/month)	–	220
	Deep water capacity (mm)	–	320
	Deep conductivity (mm/month)	–	750
	Runoff resistance factor (includes LAI)	–	3.8
GR4J	X1	Maximum capacity of production store (mm)	−11.35
	X2	Groundwater exchange coefficient (mm)	3.25
	X3	Maximum capacity of routing store (mm)	6.85
	X4	Time peak ordinate of unit hydrograph (day)	2.15
HBV	Ko	Recession coefficient (d^{-1})	0.29
	K1	Recession coefficient (d^{-1})	0.25
	K2	Recession coefficient (d^{-1})	0.05
	UZL	Threshold for Ko outflow (mm)	80
	MAXBAS	Routing, length of weighting Function (d)	4
	FC	Maximum soil moisture (mm)	400
	BETA	Shape coefficient	4
SWAT	CN2	runoff curve number	77.80
	Alpha_bf	Base flow alpha factor (days)	0.75
	Gw_delay	Groundwater delay time (days)	250
	Gwqmn	Threshold depth of water in the shallow aquifer required (mm)	1.46
	GW_revap	Groundwater coefficient	0.1945
	Esco	Soil evaporation compensation factor	0.99
	Ch_n2	Manning's “n” value for the main channel	0.145
	Ch_k2	Effective hydraulic conductivity in main channel alluvium (mm/hr)	98
	Sftmp	Snowfall temperature (degree centigrade)	4

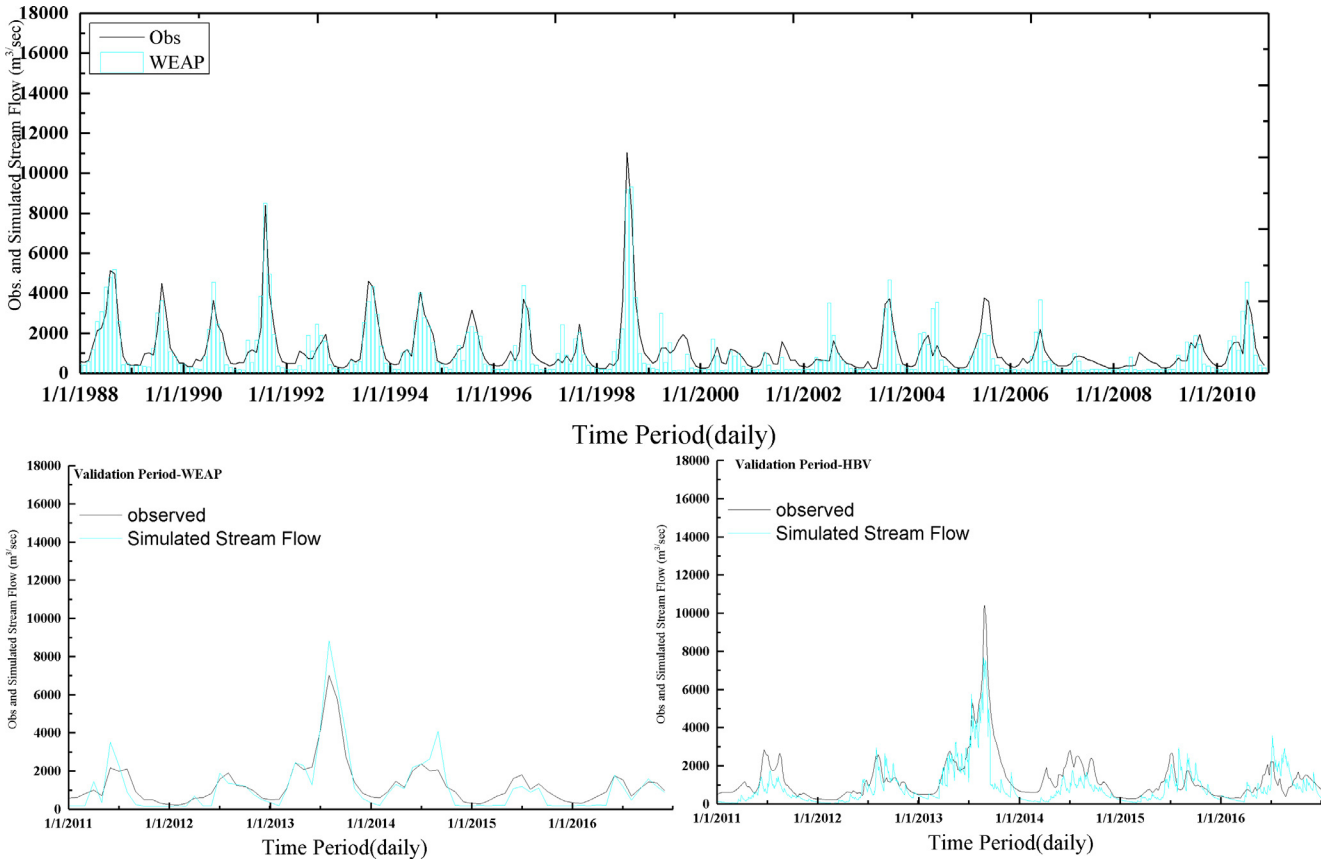

Fig. 7. Stream flow calibration and validation for the period of 1988–2016 by WEAP model.

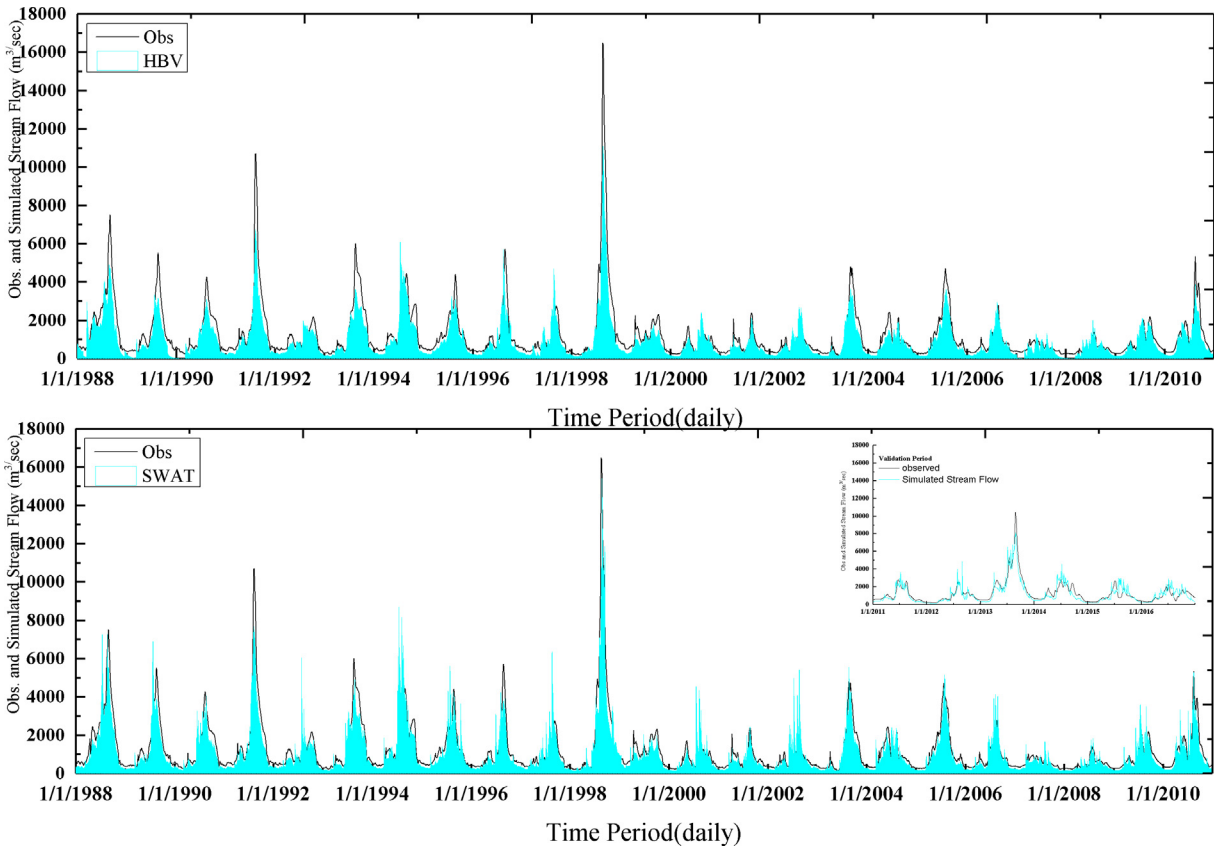

Fig. 8. Stream flow calibration and validation for the period of 1988–2016 by SWAT and HBV models.

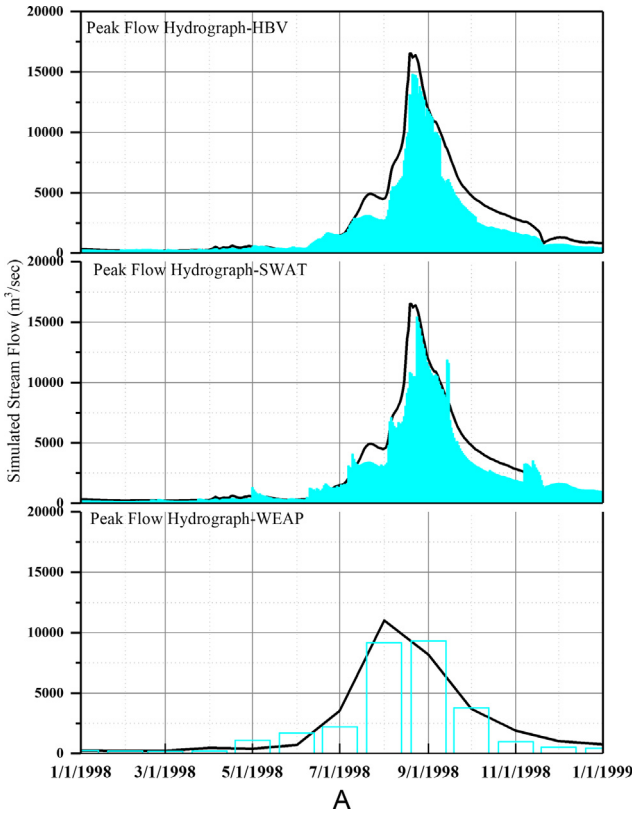

Fig. 9. Peak flow hydrographs captured by HBV, SWAT and WEAP models.

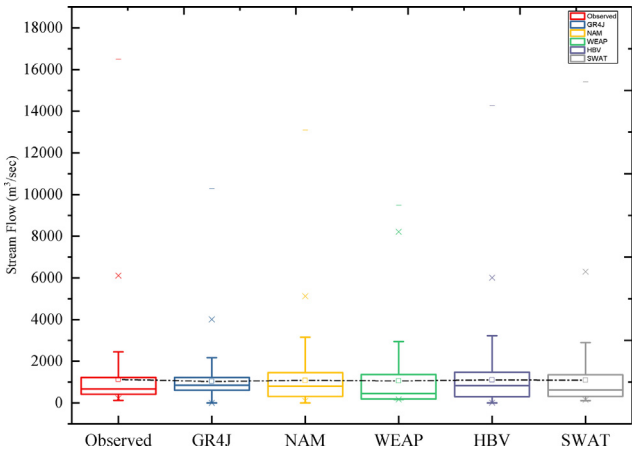

Fig. 10. Comparison between hydrological models forced by corrected precipitation.

overland flow runoff coefficient, Lmax and CK1K2 were the most sensitive and had the most influence on the process of predicting discharge. For instance, it was revealed that increasing the Lmax value tends to decrease the simulated accumulated volume as well as decrease in the simulated hydrograph peak and vice versa. The overland flow runoff coefficient, which divides the excess rainfall into overland flow and infiltration, also had a substantial effect in this case. The coefficient value close to zero showed a drastic decrease in the overland flow volume while a value close to or greater than 0.3 demonstrated the best agreement between simulated and observed discharges. CK1,2 generally controls the hydrograph peak. The analysis found that the most suitable value of CK1,2 was 16 showing the most appropriate match for predicting the discharge amount. The optimized calibrated values for models are presented in Table 6. Moreover, NAM model captured the peak flow hydrograph better than the GR4J model (Fig. 6).

(b) **Semi-distributed and distributed hydrological models**: The evaluation of semi-distributed and distributed hydrological model at the time of calibration and validation for the period of 1988 to 2016 is presented in Figs. 7 & 8. The WEAP model was auto-calibrated by the Parameter Estimation Tool. The NSE value for the period from 1988 to 2010 was 0.83, while during the validation period the values were never less than 0.88. The high NSE values could be caused by the maximum variables of the input data (precipitation, temperature, etc.) and by the fact that there was less variation in this data, compare to daily input data. During the calibration process, soil water capacity and deep conductivity were found to be the most sensitive parameters which directly affect the hydrograph peak. The HBV model ran for the same period and the NSE value was found 0.80, while during the validation period the NSE value was never less than 0.82. During analysis, it was observed that parameters such as MAXBAS, K1, and UZL, were most influencing on high flow than the volume balance. Especially, K1, Ko and UZL that control interflow and overland flow. The influence of these parameters on catchment in the form of changing of peak flow hydrograph. Abebe et al. (2010) studied the sensitivity function of HBV model in the Leaf River watershed of United States and concluded that parameters from transformation routine (i.e., MAXBAS, Ko, K1, and UZL) directly influence the peak flows. For SWAT model, calibration of stream flow was done on daily time steps for the period of 1988 to 2010. The model well simulated the stream flow in the entire catchments. The best NSE value was found 0.81, while for validation period (2011–2016) the NSE value was never less than 0.80. The calibration was done considering sensitive flow parameter that are described in Table 6. For realistic simulation of stream flow, the model parameters were manually adjusted, and this procedure continued until the best values were obtained. During the analysis, the model parameters that directly influenced the surface runoff such as curve number Cn2, soil water capacity (Sol_Awc), and evaporation factor (Esco), respectively. High value of curve number reduces the base flow and increases the surface runoff, while Sol_Awc has inverse relation with hydric balance. For example, high value of Sol_Awc reduces the amount of available water for percolation and surface runoff because high Sol_Awc helps the soil maintain its humidity. The correlation coefficient for distributed and semi-distributed model was never less than 0.80 found during the whole simulation compared to observed stream flow Table 5. Moreover, the semi-distributed and distributed models well captured the peak flow compared to lumped models (Fig. 9). This also suggested that consideration of distributed characteristics of land use, geology, topography is necessary for well assessment of hydrological process.

4.4. Comparison between hydrological models (GR4J, WEAP, NAM, HBV, and SWAT)

With the WEAP model, the best NSE value for the validation period was 0.88. Similarly, for the HBV and SWAT models it was 0.82 and 0.80, while for lumped models i.e. NAM and GR4J, the NSE value was 0.80, and 0.64, respectively. The hydrological models could not determine the origin of runoff in a reliable manner. As a result, it is necessary to compare the performance of hydrological models by a sensitive climatic input parameter such as precipitation. For this purpose, we employed 1988 to 2010 as a trial period based on an ensemble of corrected precipitation from seven GCMs and other climatic parameters remained the same as the input in each model to evaluate the performance of hydrological models. The percentage change in the variation of discharge that was calculated from five hydrological models based on forcing an ensemble of GCMs are presented in Fig. 10. The results show that the change in variation in predicted discharge by SWAT was −3%

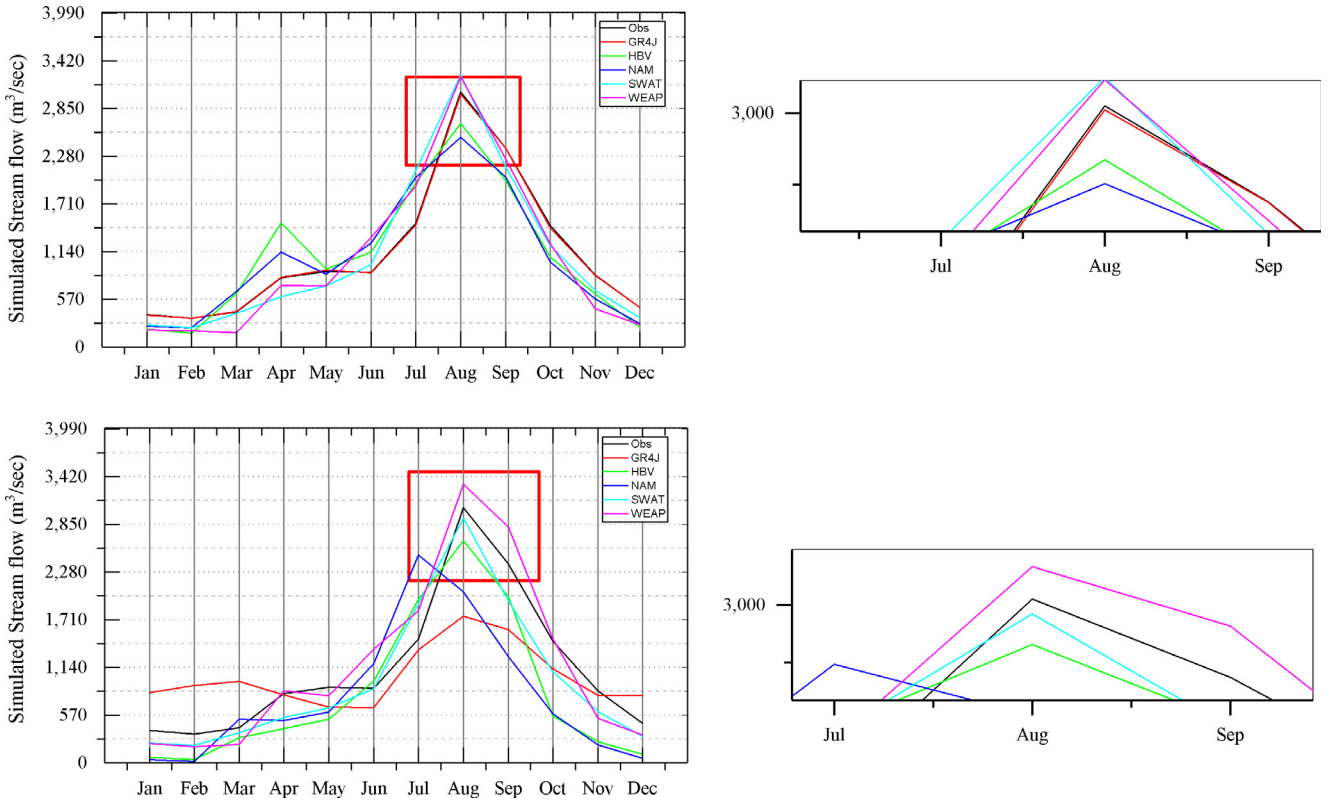

Fig. 11. Performance of bias correction methods based on long-term mean monthly stream flow; upper (quantile mapping) lower (linear scaling).

(QM) and −13% (Linear scaling), while those for HBV, WEAP, NAM, and GR4J were −2% & −25%, −6% & +3%, −4% & −29%, −7% & −29%, respectively, when compared with observed discharge under the same conditions. The large reduction of projected discharge by models may have been associated with the bias correction method, but models performed satisfactory when corrected precipitation by quantile method is used.

The SRB experiences a harsh environment such as long, cold winters with snow and short summers with days of heavy rain. This was the first time these hydrological models have been used in this environment. The satisfactory performance of GR4J based on NSE statistics is caused by its limitations as pointed by Perrin et al. (2003). For example, model does not work well when some key processes are active on a catchment such as if the catchment is significantly influenced by snow, karstic influences, catchment with dams, and dry environments since the rainfall-runoff relationship is much more non-linear. Merz et al. (2009) study the scale effects in conceptual hydrological modeling and concluded that some parameters may not be well estimated due to larger uncertainties that are associated with internal state variables. The SWAT, HBV, WEAP and NAM models displayed good performance in the SRB, which was confirmed by the NSE values of greater than 0.80, respectively.

To analyze the performance of bias correction methods, the long term monthly average was also taken for simulated stream flow Fig. 11. The results revealed that hydrological models forced by bias correction of GCMs with quantile mapping well captured the peak flow of August, only NAM and HBV under estimated the peak flow. In contrast, the stream flow simulation based on precipitation extracted from ensembles of GCMs that were corrected with linear scaling failed in capturing satisfactory peak flow. The simulated stream flow was showing more spread in the winter months (Jan, Feb) compared to summer months. The peak flow curve with respect to base flow indicated that lumped models failed to capture peak flow compared to semi distributed and distributed models.

4.5. *Projection of precipitation and stream flow for the period of 2070–2099 under RCP 8.5*

The projected precipitation and stream flow variations for the period of 2070 to 2099 is presented in Fig. 12. For this purpose, GCMs under high emission scenario i.e. RCP 8.5 were used. The radiating forcing in this scenario was expected to increase by 8.5 $W m^{-2}$ at the end of 21st century compared to other pathways (Taylor et al., 2012). Based on results (Section 4.4), the bias in the GCMs were corrected with quantile mapping method, because this method showed good agreement with observations compared to linear scaling. The results based on Sen's slope estimator (Sen, 1968) revealed that precipitation expected to increase 1.56 mm/year. The simulated monthly-corrected precipitation plotted against the corresponding base line period 1961 to 1990 suggest that models are able to predict realistic precipitation cycle. Most of the models well produced the single peak. The maximum precipitation was predicted in the summer season except CanCM4 and CCSM4. The previous studies also documented that precipitation trend increases in the basin (Sun et al., 2015; Wang and Chen, 2014). Furthermore, the hydrological models were forced by predicted precipitation to estimate the variation in stream flow for far-future period (2071–2099). The results exhibited that maximum increase in stream flow, WEAP +25% and minimum +3% (GR4J) found with respect to base line period (1988–2016).

4.6. *Uncertainties*

In climate change and hydrological impact studies, there are number of uncertainties which are associated with quality of data and method used including model structure and parameters (Bosshard et al., 2013; Leng et al., 2015). In this study, historical outputs of GCMs from CMIP5 and GCMs under RCP 2.6 and 8.5 were used to analyze the differences and comparison between hydrological models. Although the GCMs were converted into common resolution of (0.5° × 0.5°) and

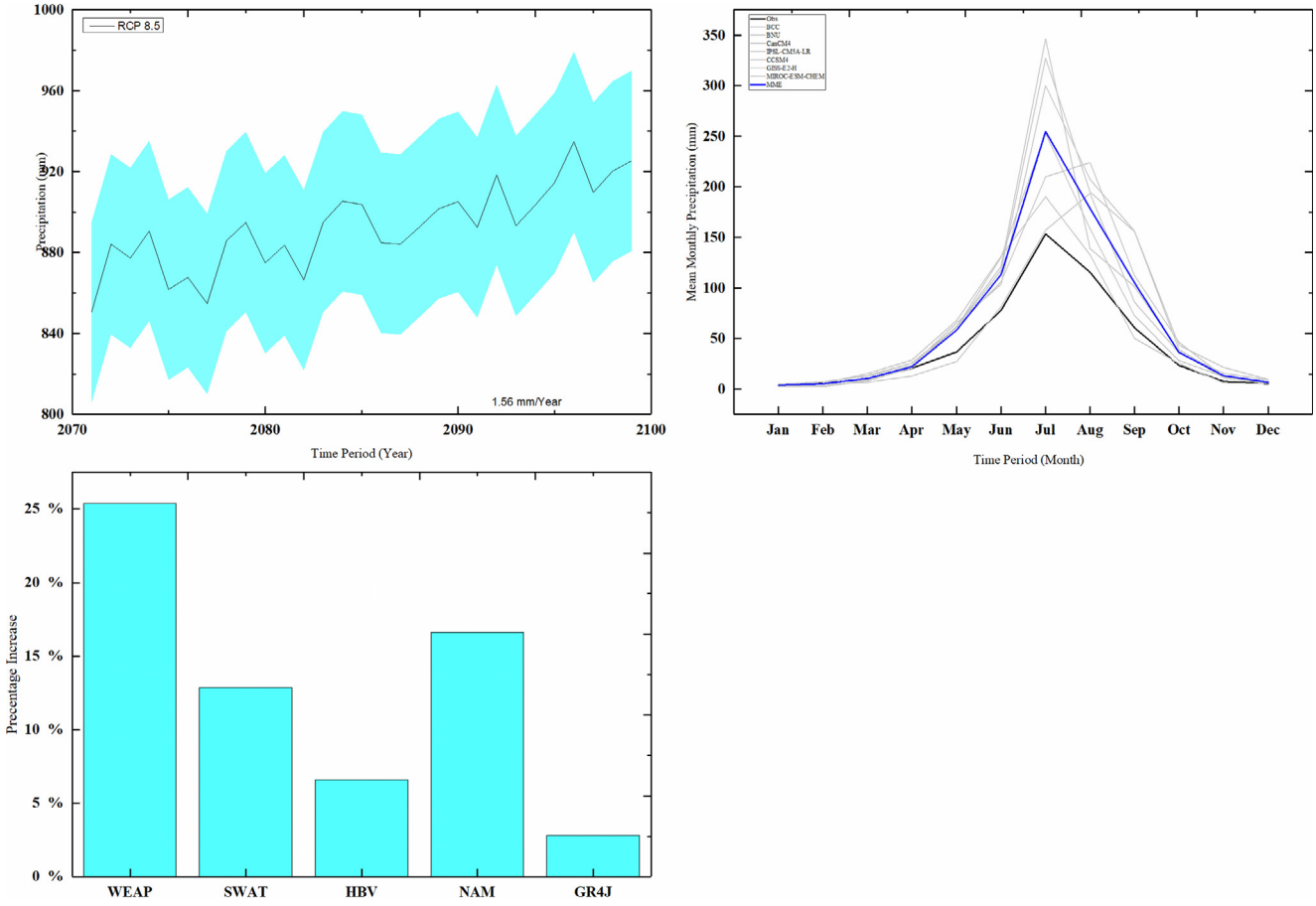

Fig. 12. Future projection of (a) precipitation, (b) mean monthly stream flow c) percentage variation capture by hydrological models for the period of 2071–2099 in the SRB.

biases were corrected with linear scaling and quantile mapping methods, but the accuracy was still uncertain. The uncertainties related to hydrological models also influenced on the climate impact studies. Although different hydrological models were used to assess the stream flow variation in the basin but reliability of input data is important for accurate reflection of hydrological conditions. For example, digital elevation model, soil map, and land use maps have a resolution of 1 km, which may not represent the parameters' heterogeneity. Moreover, agricultural and human management practices that have a significant effect on stream flow could be considered for comprehensive planning of water resources as well as to understand the hydrological process of the basin. In addition, to limitations and uncertainties, the novelty of this study is application of multiple hydrological models, GCMs and bias correction methods were used to assess the variation in stream flow.

5. Conclusions

In this article, the hydrological models (GR4J, WEAP, NAM, HBV, and SWAT) and GCMs were used in the SRB. The performances of GCMs were evaluated by bias correction methods. The quantile mapping and linear scaling methods were used to translate GCMs outputs at the site scale. In this study, for GCMs precipitation simulations, daily and monthly scale factors were used to improve the daily variation in precipitation. Furthermore, hydrological models were forced by precipitation from an ensemble of bias corrected GCMs. The performance of the hydrological models were evaluated by correlation coefficient and NSE criteria.

To evaluate the GCMs, seven GCMs (BCC-CSM 1.1 (m), BNU-ESM, CanESM2, IPSL-CM5A-LR, GISS-E2-H, CCSM4, and MICRO-ESM-CHEM) were obtained covering the SRB. Moreover, statistical indicators and graphical representation were also used for evaluation period (1961–1990). Before applying the bias correction method, raw GCMs were plotted against the observational data. The results showed that none of GCM performed better against the observational data. After applying the modified bias correction (in which daily scale factors were obtained) and quantile mapping method, an improvement was observed in all statistical indicators. In comparison with the bias correction method (in which monthly scale factors were obtained) less improvement was observed than with the modified linear scaling and quantile mapping bias correction method.

To evaluate the hydrological models, the models were forced by using both observed and bias corrected precipitation data. When analyzing the performance of the models using observed precipitation data, the final correlation coefficient and NSE criterion values were found for the WEAP (0.86, and 0.83), the GRJ4 (0.67, and 0.62), the NAM (0.80, and 0.73), the HBV (0.86 and 0.80), and the SWAT (0.82 and 0.81), respectively. However, with bias corrected precipitation data, the results showed variation and changes in the predicted discharge amounts by the SWAT (−3% & −13%), while results for the HBV (−2% & −25%), NAM (−4% & −29%), GR4J (−7% & −29%), and WEAP (−6% & +3%), were comparable to the observed predicted discharge amounts. The differences in projection of discharge may be related to biases of the GCMs or usage of bias correction method. Moreover, the projected precipitation results revealed that precipitation expected to increase 1.56 mm/year and stream flow 3% to 25% with respect to base line for the period of 2071–2099. In summary, this study stresses that hydrological models contribute notably to the variations in the projection of discharge in the SRB. Therefore, future studies should consider employing multiple hydrological models instead of using single

model to conduct future planning and management of agricultural activities and water resources.

Acknowledgements

This work was supported by the National Natural Science Foundation of China (Grant Nos. 51579044, 41071053, and 51479032), the Specialized Research Fund for Innovative Talents of Harbin (Excellent Academic Leader; Grant No. 2013RFXXJ001), and the Science and Technology Program of Water Conservancy of Heilongjiang Province (Grant Nos. 201319, 201501, and 201503). We thank LetPub (www.letpub.com) for its linguistic assistance during the preparation of this manuscript.

References

Abebe, N.A., Ogden, F.L., Pradhan, N.R., 2010. Sensitivity and uncertainty analysis of the conceptual HBV rainfall-runoff model: implications for parameter estimation. J. Hydrol. 389, 301–310. https://doi.org/10.1016/j.jhydrol.2010.06.007.

Bi, H., Liu, B., Wu, J., Yun, L., Chen, Z., Cui, Z., 2009. Effects of precipitation and landuse on runoff during the past 50 years in a typical watershed in Loess Plateau, China. Int. J. Sediment Res. 24, 352–364. https://doi.org/10.1016/S1001-6279(10)60009-1.

Bosshard, T., Carambia, M., Goergen, K., Kotlarski, S., Krahe, P., Zappa, M., Schär, C., 2013. Quantifying uncertainty sources in an ensemble of hydrological climate-impact projections. Water Resour. Res. 49, 1523–1536. https://doi.org/10.1029/2011WR011533.

Chatfield, C., 2016. The Analysis of Time Series: An Introduction. CRC Press.

Chen, H., Xu, C.-Y., Guo, S., 2012. Comparison and evaluation of multiple GCMs, statistical downscaling and hydrological models in the study of climate change impacts on runoff. J. Hydrol. 434–435, 36–45. https://doi.org/10.1016/j.jhydrol.2012.02.040.

Fang, G.H., Yang, J., Chen, Y.N., Zammit, C., 2015. Comparing bias correction methods in downscaling meteorological variables for a hydrologic impact study in an arid area in China. Hydrol. Earth Syst. Sci. 19, 2547–2559. https://doi.org/10.5194/hess-19-2547-2015.

Fang, N.F., Shi, Z.H., Li, L., Guo, Z.L., Liu, Q.J., Ai, L., 2012. The effects of rainfall regimes and land use changes on runoff and soil loss in a small mountainous watershed. Catena 99, 1–8. https://doi.org/10.1016/j.catena.2012.07.004.

Faiz, M.A., Liu, D., Fu, Q., Qamar, M.U., Dong, S., Khan, M.I., Li, T., 2017a. Complexity and trends analysis of hydrometeorological time series for a river streamflow: A case study of Songhua River Basin, China. River Res. Appl. https://doi.org/10.1002/rra.3236.

Faiz, M.A., Liu, D., Fu, Q., Uzair, M., Khan, M.I., Baig, F., Li, T., Cui, S., 2017b. Stream flow variability and drought severity in the Songhua River Basin, Northeast China. Stoch. Environ. Res. Risk Assess. https://doi.org/10.1007/s00477-017-1463-3.

Faiz, M.A., Liu, D., Fu, Q., Wrzesiński, D., Baig, F., Nabi, G., Cui, S., 2018. Extreme precipitation and drought monitoring in northeastern China using general circulation models and pan evaporation-based drought indices. Clim. Res. 74 (3), 231–250.

Giuntoli, I., Vidal, J.-P., Prudhomme, C., Hannah, D.M., 2015. Future hydrological extremes: the uncertainty from multiple global climate and global hydrological models. Earth Syst. Dyn. 6, 267.

Gosling, S., Taylor, R.G., Arnell, N., Todd, M.C., 2011. A comparative analysis of projected impacts of climate change on river runoff from global and catchment-scale hydrological models. Hydrol. Earth Syst. Sci. 15, 279–294.

Gudmundsson, L., Bremnes, J.B., Haugen, J.E., Engen-Skaugen, T., 2012. Technical note: downscaling RCM precipitation to the station scale using statistical transformations; a comparison of methods. Hydrol. Earth Syst. Sci. 16, 3383–3390. https://doi.org/10.5194/hess-16-3383-2012.

Hagemann, S., Chen, C., Clark, D., Folwell, S., Gosling, S.N., Haddeland, I., Hannasaki, N., Heinke, J., Ludwig, F., Voss, F., 2013. Climate change impact on available water resources obtained using multiple global climate and hydrology models. Earth Syst. Dyn. 4, 129–144.

Hay, L.E., Clark, M.P., 2003. Use of statistically and dynamically downscaled atmospheric model output for hydrologic simulations in three mountainous basins in the western United States. J. Hydrol. 282, 56–75.

Hessami, M., Gachon, P., Ouarda, T.B.M.J., St-Hilaire, A., 2008. Automated regression-based statistical downscaling tool. Environ. Model. Softw. 23, 813–834.

IPCC, 2014. Summary for policymakers. In: Field, Christopher B., Barros, Vicente R., Mastrandrea, Michael D., Mach, Katharine J., Abdrabo, M.A.-K. Adger, Anokhin, N., Anisimov, Yury A., Arent, Oleg A., Barnett, Douglas J. (Eds.), Climate Change 2014: Impacts, Adaptation, and Vulnerability. Part A: Global and Sectoral Aspects. Contribution of Working Group II to the Fifth Assessment Report of the Intergovernmental Panel on Climate Change. Cambridge University Press, pp. 1–32.

Jakob Themeßl, M., Gobiet, A., Leuprecht, A., 2011. Empirical-statistical downscaling and error correction of daily precipitation from regional climate models. Int. J. Climatol. 31, 1530–1544. https://doi.org/10.1002/joc.2168.

Jiang, T., Chen, Y.D., Xu, C., Chen, X., Chen, X., Singh, V.P., 2007. Comparison of hydrological impacts of climate change simulated by six hydrological models in the Dongjiang Basin, South China. J. Hydrol. 336, 316–333.

Khan, M.S., Coulibaly, P., 2010. Assessing hydrologic impact of climate change with uncertainty estimates: Bayesian Neural Network Approach. J. Hydrometeorol. 11, 482–495. https://doi.org/10.1175/2009JHM1160.1.

Khan, M.I., Liu, D., Fu, Q., Dong, S., Liaqat, U.W., Faiz, M.A., Hu, Y., Saddique, Q., 2016. Recent climate trends and drought behavioral assessment based on precipitation and temperature data series in the Songhua river basin of china. Water Resour. Manag. 30 (13), 4839–4859.

Laugel, A., Menendez, M., Benoit, M., Mattarolo, G., Méndez, F., 2014. Wave climate projections along the French coastline: Dynamical versus statistical downscaling methods. Ocean Model. https://doi.org/10.1016/j.ocemod.2014.09.002.

Lee Rodgers, J., Nicewander, W.A., 1988. Thirteen ways to look at the correlation coefficient. Am. Stat. 42, 59–66.

Lenderink, G., Buishand, A., van Deursen, W., 2007. Estimates of future discharges of the river Rhine using two scenario methodologies: direct versus delta approach. Hydrol. Earth Syst. Sci. 11, 1145–1159.

Leng, G., Tang, Q., Rayburg, S., 2015. Climate change impacts on meteorological, agricultural and hydrological droughts in China. Glob. Planet. Change 126, 23–34.

Lerat, J., Perrin, C., Andréassian, V., Loumagne, C., Ribstein, P., 2012. Towards robust methods to couple lumped rainfall-runoff models and hydraulic models: a sensitivity analysis on the Illinois River. J. Hydrol. 418–419, 123–135. https://doi.org/10.1016/j.jhydrol.2009.09.019.

Li, J., Zhang, Q., Chen, Y.D., Singh, V.P., 2013. GCMs-based spatiotemporal evolution of climate extremes during the 21st century in China. J. Geophys. Res. Atmos. 118.

Liu, D., Luo, M., Fu, Q., Zhang, Y., Imran, K.M., Zhao, D., Li, T., Abrar, F.M., 2016. Precipitation complexity measurement using Multifractal spectra empirical mode decomposition Detrended fluctuation analysis. Water Resour. Manag. 30, 505–522.

Mahmood, R., Babel, M.S., 2013. Evaluation of SDSM developed by annual and monthly sub-models for downscaling temperature and precipitation in the Jhelum basin, Pakistan and India. Theor. Appl. Climatol. 113, 27–44.

Mahmood, R., Shaofeng, J.I.A., 2016. An extended linear scaling method for downscaling temperature and its implication in the Jhelum River basin, Pakistan, and India, using CMIP5 GCMs. Theor. Appl. Climatol. 1–10.

Maraun, D., Wetterhall, F., Chandler, R.E., Kendon, E.J., Widmann, M., Brienen, S., Rust, H.W., Sauter, T., Themeßl, M., Venema, V.K.C., Chun, K.P., Goodess, C.M., Jones, R.G., Onof, C., Vrac, M., Thiele-Eich, I., 2010. Precipitation downscaling under climate change: recent developements to bridge the gap between dynamical models and the end user. Rev. Geophys. 48, 1–38. https://doi.org/10.1029/2009RG000314.1.INTRODUCTION.

Merz, R., Parajka, J., Blöschl, G., 2009. Scale effects in conceptual hydrological modeling. Water Resour. Res. 45. https://doi.org/10.1029/2009WR007872.

Mitchell, et al., 1966. Climatic change. WMO Technical Note, 79 (WMO-No. 195/TP. 100). World Meteorol. Organ. Geneva.

Mu, X., Li, Y., Gao, P., Shao, H., Wang, F., 2012. The runoff declining process and water quality in Songhuajiang River catchment, China under global climatic change. CLEAN–Soil Air, Water 40, 394–401.

Nash, J.E., Sutcliffe, J.V., 1970. River flow forecasting through conceptual models part I—A discussion of principles. J. Hydrol. 10, 282–290.

Perrin, C., Michel, C., Andréassian, V., 2003. Improvement of a parsimonious model for streamflow simulation. J. Hydrol. 279, 275–289.

Piani, C., Haerter, J.O., Coppola, E., 2010a. Statistical bias correction for daily precipitation in regional climate models over Europe. Theor. Appl. Climatol. 99, 187–192.

Piani, C., Weedon, G.P., Best, M., Gomes, S.M., Viterbo, P., Hagemann, S., Haerter, J.O., 2010b. Statistical bias correction of global simulated daily precipitation and temperature for the application of hydrological models. J. Hydrol. 395, 199–215. https://doi.org/10.1016/j.jhydrol.2010.10.024.

Pokhrel, B.K., Chevallier, P., Andréassian, V., Tahir, A.A., Arnaud, Y., Neppel, L., Bajracharya, O.R., Budhathoki, K.P., 2014. Comparison of two snowmelt modelling approaches in the Dudh Koshi basin (eastern Himalayas, Nepal). Hydrol. Sci. J. 59, 1507–1518.

Poulin, A., Brissette, F., Leconte, R., Arsenault, R., Malo, J.-S., 2011. Uncertainty of hydrological modelling in climate change impact studies in a Canadian, snow-dominated river basin. J. Hydrol. 409, 626–636.

Rogelj, J., Meinshausen, M., Knutti, R., 2012. Global warming under old and new scenarios using IPCC climate sensitivity range estimates. Nat. Clim. Chang. 2, 248.

Semenov, M.A., Barrow, E.M., 1997. Use of a stochastic weather generator in the development of climate change scenarios. Clim. Change 35, 397–414.

Sen, P.K., 1968. Estimates of the regression coefficient based on Kendall's tau. J. Am. Stat. Assoc. 63, 1379–1389.

Song, X., Song, S., Sun, W., Mu, X., Wang, S., Li, J., Li, Y., 2015. Recent changes in extreme precipitation and drought over the Songhua River Basin, China, during 1960–2013. Atmos. Res. 157, 137–152.

Sun, F., Roderick, M.L., Lim, W.H., Farquhar, G.D., 2011. Hydroclimatic projections for the Murray-Darling Basin based on an ensemble derived from Intergovernmental Panel on Climate Change AR4 climate models. Water Resour. Res. 47. https://doi.org/10.1029/2010WR009829.

Sun, Q., Miao, C., Duan, Q., 2015. Projected changes in temperature and precipitation in ten river basins over China in 21st century. Int. J. Climatol. 35, 1125–1141.

Taylor, K.E., 2001. Summarizing multiple aspects of model performance in a single diagram. J. Geophys. Res. Atmos. 106, 7183–7192.

Taylor, K.E., Stouffer, R.J., Meehl, G.A., 2012. An overview of CMIP5 and the experiment design. Bull. Am. Meteorol. Soc. 93, 485–498. https://doi.org/10.1175/BAMS-D-11-00094.1.

Teklesadik, A.D., Alemayehu, T., van Griensven, A., Kumar, R., Liersch, S., Eisner, S., Tecklenburg, J., Ewunte, S., Wang, X., 2017. Inter-model comparison of hydrological impacts of climate change on the Upper Blue Nile basin using ensemble of hydrological models and global climate models. Clim. Change 141, 517–532.

Teutschbein, C., Seibert, J., 2012. Bias correction of regional climate model simulations

for hydrological climate-change impact studies: review and evaluation of different methods. J. Hydrol. 456, 12–29.
Tian, T., Boberg, F., Christensen, O.B., Christensen, J.H., She, J., Vihma, T., 2013. Resolved complex coastlines and land-sea contrasts in a high-resolution regional climate model: a comparative study using prescribed and modelled SSTs Tellus. Ser. A Dyn. Meteorol. Oceanogr. 65. https://doi.org/10.3402/tellusa.v65i0.19951.
Wang, L., Chen, W., 2014. A CMIP5 multimodel projection of future temperature, precipitation, and climatological drought in China. Int. J. Climatol. 34, 2059–2078.
Wetterhall, F., Bárdossy, A., Chen, D., Halldin, S., Xu, C., 2006. Daily precipitation-downscaling techniques in three Chinese regions. Water Resour. Res. 42.
Wilby, R.L., Charles, S.P., Zorita, E., Timbal, B., Whetton, P., Mearns, L.O., 2004. Guidelines for use of climate scenarios developed from statistical downscaling methods. Support. Mater. to Intergov. Panel Clim. Chang. 27.
Wilby, R.L., Hay, L.E., Gutowski, W.J., Arritt, R.W., Takle, E.S., Pan, Z., Leavesley, G.H., Clark, M.P., 2000. Hydrological responses to dynamically and statistically downscaled climate model output. Geophys. Res. Lett. 27, 1199–1202.
Yin, J., He, F., Jiu Xiong, Y., Yu Qiu, G., 2017. Effects of land use/land cover and climate changes on surface runoff in a semi-humid and semi-arid transition zone in northwest China. Hydrol. Earth Syst. Sci. 21, 183–196. https://doi.org/10.5194/hess-21-183-2017.